Hemoglobin Can Attenuate Hydrogen Peroxide–Induced Oxidative Stress by Acting as an Antioxidative Peroxidase

Corinne C. Widmer,[1] Claudia P. Pereira,[1] Peter Gehrig,[2] Florence Vallelian,[1] Gabriele Schoedon,[1] Paul W. Buehler,[3] and Dominik J. Schaer[1]

Abstract

Hemoglobin is considered a potentially toxic molecule when released from erythrocytes during hemolysis, inflammation, or tissue injury. The mechanisms of toxicity involve reduced nitric oxide bioavailability and oxidative processes both occurring at the heme prosthetic groups. When the endogenous oxidant H_2O_2 reacts with Hb, transient radicals are generated during the peroxidative consumption of H_2O_2. If not neutralized, these radicals can lead to tissue toxicity. The net biologic effect of extracellular Hb in an H_2O_2-rich environment will therefore be determined by the balance of H_2O_2 decomposition (potential protective effect) and radical generation (potential damaging effect). Here we show that Hb can protect different cell types from H_2O_2-mediated cell death and the associated depletion of intracellular glutathione and ATP. Importantly, Hb blunts the transcriptional oxidative-stress response induced by H_2O_2 in human vascular smooth muscle cells (VSMCs). Based on spectrophotometric and quantitative mass spectrometry analysis, we suggested a novel mechanism in which Hb redox-cycles H_2O_2 and simultaneously internalizes the radical burden, with irreversible structural globin changes starting with specific amino acid oxidation involving the heme proximate βCys93 and ultimately ending with protein precipitation. Our results suggest that complex interactions determine whether extracellular Hb, under certain circumstances, acts a protective or a damaging factor during peroxidative stress conditions. *Antioxid. Redox Signal.* 12, 185–198.

Introduction

HEMOGLOBIN (Hb) is released from red blood cells (RBCs) during intravascular hemolysis or on extravasation and subsequent lysis of RBCs during micro- or macroscopic tissue injury. Extracellular Hb has been implicated in the pathogenesis of hemolytic diseases such as sickle cell anemia or malaria and also in more localized processes such as in atherosclerosis with associated intraplaque hemorrhage (1, 6, 8, 18, 22, 35). Two major processes have been explored to explain the pathophysiologic activity of Hb. The neutralization of nitric oxide by the dioxygenase reaction is likely to be involved in the vasoconstrictive and hypertensive properties of Hb (34). Peroxidative properties of Hb, when it reacts with physiologic oxidants such as hydrogen peroxide, have been advocated to propagate oxidative cell and tissue damage. The *in vivo* examples of the oxidative activity of Hb can be found with large intravascular Hb exposures, which cause lipid peroxidation and subsequent lipid peroxide protein modification in the kidneys of exposed animals (4). The excretion of oxidatively modified Hb in the urine of these animals sug-
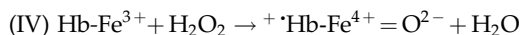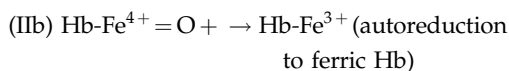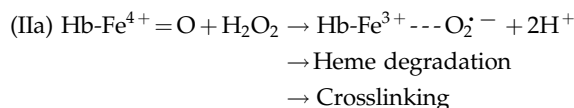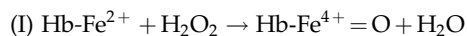
gests that Hb is directly involved in the processes leading to parenchymal damage (7). In addition, free heme or Hb oxidation products or both have been shown to propagate inflammatory reactions and to enhance cellular susceptibility to oxidative stress (3, 17, 24).

The oxidative toxicity of Hb or myoglobin (Mb) has been associated with the generation of protein radicals, which are formed when ferric (Fe^{3+}) Hb reacts with H_2O_2 in the following reaction: $Hb\text{-}Fe^{3+} + H_2O_2 \rightarrow {}^{\cdot}Hb\text{-}Fe^{4+} = O + H_2O$ (32, 33). While H_2O_2 is consumed during this reaction, the formed radicals can abstract hydrogen atoms from the environment and thereby initiate oxidative damage. In cell cultures, the reaction of ferric myoglobin or some chemically modified Hbs with low and continuous concentrations of H_2O_2 enhanced apoptosis compared with the effect of H_2O_2 or myoglobin alone (12, 13). Under physiologic conditions, however, it is unlikely that intravascular or extravascular Hb is exclusively in its ferric oxidative state when subjected to H_2O_2. Therefore, the more complicated and less well established reaction of ferrous or a mixed ferric/ferrous Hb reaction with H_2O_2 might be a more realistic process *in vivo*. In

[1]Division of Internal Medicine, University Hospital, and [2]Functional Genomics Center Zurich, University of Zurich and Swiss Federal Institute of Technology, Zurich, Switzerland.
[3]Center for Biologics Evaluation and Research (CBER), U.S. Food and Drug Administration, Bethesda, Maryland.

the initial reaction of ferrous Hb, H_2O_2 is consumed, resulting in the formation oxo-ferryl Hb (Hb-Fe$=$O). No heme- or protein-located radical is formed during this initial reaction. The reactions of ferrous Hb with H_2O_2 can be summarized as follows (9, 21, 28–30).

$$\text{(I) Hb-Fe}^{2+} + H_2O_2 \rightarrow \text{Hb-Fe}^{4+} = O + H_2O$$
$$\text{(IIa) Hb-Fe}^{4+} = O + H_2O_2 \rightarrow \text{Hb-Fe}^{3+} \text{---} O_2^{\bullet -} + 2H^+$$
$$\rightarrow \text{Heme degradation}$$
$$\rightarrow \text{Crosslinking}$$
$$\text{(IIb) Hb-Fe}^{4+} = O + \ \rightarrow \text{Hb-Fe}^{3+} \text{ (autoreduction}$$
$$\text{to ferric Hb)}$$
$$\text{(IV) Hb-Fe}^{3+} + H_2O_2 \rightarrow {}^{+\bullet}\text{Hb-Fe}^{4+} = O^{2-} + H_2O$$

The biologic consequences of a heme-protein reaction in H_2O_2-rich environments are likely a result of the balance of H_2O_2 consumption (antioxidative protection) and, conversely, the production of free radicals (oxidative damage). However, in light of the cytotoxic nature of the reaction of H_2O_2 with Mb and with some chemically modified Hbs (developed as blood substitutes), the H_2O_2 consumption or peroxidase activity has not been considered an intrinsic antioxidant activity of Hb. We recently found extensive heme degradation, α-globin cross-linking, and a specific pattern of β-globin amino acid oxidations that result from the reaction of ferrous Hb with H_2O_2 (7, 21, 42). These structural changes occurring during the reaction of Hb with H_2O_2 are likely a result of heme-derived radicals reacting with globin amino acids and porphyrin, respectively. In theory, these reactions could "absorb" a significant amount of radical-derived oxidative impact and thereby protect the physiologic environment.

In this study, we found that cell-free Hb can protect different cell types from H_2O_2-induced oxidative stress and associated cell damage. The extensive oxidative modification of Hb, which involves globin-chain amino acid oxidation and protein precipitation, is compatible with a protective activity of Hb involving "internalization" of heme-associated oxidative processes.

Materials and Methods

Glucose oxidase (GOX; 200 units/mg protein or more) and catalase (4,000–8,000 units/mg protein) from *Aspergilus niger* were obtained from Sigma (St. Louis, MO). Different GOX/catalase concentrations were achieved by dilution of the stock solution directly into the appropriate medium. Highly purified hemoglobin (HbA0; purity >99%, referred to as Hb) was provided by Hemosol, Inc. (Toronto, Ontario, Canada) and stored at –80°C until the time of use. This ultrapure Hb has been characterized extensively and is free of catalase (5). For experiments using cell impedance measurements, an essentially catalase-free stroma-free human Hb was used (provided to P.W.B. by Dr. Andre Palmer, Dept. of Chemical and Biomolecular Engineering, The Ohio State University). AcriGlow 301 was purchased from Capricorn (Portland, ME). Amplex Ultra Red Hydrogen Peroxide Assay Kit was purchased from Molecular Probes (Invitrogen, Basel, Switzerland).

Measurement of H_2O_2 production

Production of H_2O_2 by GOX in the cell-culture medium was measured by adding 0.5 μl AcriGlow 301 to the reaction.

Luminescence was measured intermittently in 5-s readings for the indicated time period with a Lumat Lb 9507 Luminometer (Berthold Technologies, Regensdorf, Switzerland) at room temperature (RT). H_2O_2 accumulation in cell-culture supernatants was measured by using the Amplex Ultra Red assay according to the manufacturer's directions. In brief, 50 μl of cell-culture supernatant was mixed with the reaction solution containing 10 mM Amplex Ultra Red and 10 U/ml horseradish peroxidase in microplates. Absorbance (560 nm) was measured in a Multi-Detection Microplate Reader (SpectraMax M2; Bucher Biotec, Basel, Switzerland) after 30 min of incubation at RT, protected from light. The presence of Hb in cell culture did not affect H_2O_2 concentrations after ultrafiltration and did not change the assay results.

Analysis of hemoglobin oxidation

Spectral analysis of ferrous and ferric HbA$_0$ (Hemosol Corp., Toronto, Ontario, Canada) was performed by using a Hewlett-Packard HP-8453 rapid-scanning diode-array spectrophotometer (Agilent Technologies, Rockville, MD). Experiments were performed in sealed cuvettes equilibrated at room temperature at 37°C with 50 μM Hb (ferrous and ferric) cell-culture medium containing 4.5 g/dl glucose with (+) and without (–) calf serum and 10 mU of glucose oxidase (GOX; type X-S derived from *Aspergillus niger*, 100,000–250,000 U/g solid material; Sigma Chemical). Initial spectra were obtained before the addition of 10 mU of GOX, and then spectra were measured every 2 min for 2 h over a wavelength range of 450–700 nm. To determine the redox state of ferric and ferrous Hb over a 2-h period, 50 μM of each Hb was diluted in glucose-rich medium with a baseline sample taken and analyzed before the addition of GOX. After the initial sample, 10 mU of GOX was added, and each tube was placed in a 37°C water bath. Samples were removed and analyzed spectrophotometrically at time 0 (immediately after the addition of GOX) and then every 2 min for 30 min, followed by every 10 min (remaining 1.5 h). Each sample was analyzed before and immediately after the addition of 2 mM sodium sulfide (Na$_2$S) as a measure of ferryl Hb. The concentration of sulfhemoglobin was calculated by using the extinction coefficient 10.5 per mm at 620 nm and expressed as ferryl Hb (16).

Cell culture

Human vascular smooth muscle cells (VSMCs) were freshly isolated from human umbilical cord veins as described (25). VSMCs (passage three through six) were cultured in DMEM high glucose (4 mg/ml of glucose), without phenol red (Amimed, BioConcept, Allschwil, Switzerland) with 10% FCS, 1% L-glutamine (200 mM), 1% penicillin (10,000 U/ml), and streptomycin (10,000 U/ml). RAW 264.7 and HEK-293 cultivated in DMEM high glucose with 10% FCS and additional 2 mM L-glutamine. All cells were kept at 37°C in a humidified atmosphere with 5% CO_2. All GOX experiments were performed at reduced FCS concentrations (5%). The experiments with HEK293 cells, shown in Fig. 2, were performed under serum-free conditions. All media were without phenol red.

Cell-impedance measurements

Cell-impedance measurements to monitor adherence, spreading, proliferation, detachment, and cell death in real

time were accomplished by using the CELLligence RTCA-SP system (Roche Applied Science, Rotkreuz, Switzerland). HEK293 cells were seeded in 96-well e-plates at a density of ∼50,000 cells per well, and the indicated stimuli (in serum-free medium) were added after reaching a stable plateau phase at a normalized cell index (CI) of ∼1.0. Data of each well were recorded every 5 min. The measurement was intermittently paused to inspect cells with the microscope. Data were analyzed by using RTCA Software 1.2 (Roche Applied Science).

Measurement of intracellular-reduced glutathione and adenosine triphosphate

Intracellular glutathione (GSH) and adenosine triphosphate (ATP) levels were measured in 96-well cell-culture microplates by using the luminescence GSH-Glo and cell-viability assays from Promega, according to the manufacturer's instructions. Luminescence was measured with an integration time of 0.5 s per well with a Multi-Detection Microplate Reader.

RNA isolation and quantitative real-time polymerase chain reaction

Total RNA was purified with the RNAeasy mini kit (Qiagen, Basel, Switzerland). RNA used for microarray analysis was treated with a DNase I digestion step (Qiagen). RNA was quantified spectrophotometrically by using the Nanodrop ND-1000 spectrophotometer (NanoDrop Technologies, Wilmington, DE). Real-time two-step reverse transcription (RT)-polymerase chain reaction (PCR) was performed on a Fast Real-Time PCR System Instrument (Applied Biosystems, Rotkreuz, Switzerland) by using Taqman reverse transcription and SYBR Green master mix PCR reagents (Applied Biosystems, Roche, Switzerland). Melting-curve analysis was performed after each PCR experiment to show the specificity of amplification reactions and to exclude excessive primer-dimer formation. Temperature-cycling profiles were 10 min at 95°C, 45 cycles of 15 s at 95°C, 10 s at 55–67°C, and 13 s at 72°C. Gene-specific quantitative data were corrected for HPRT RNA abundance in the respective sample and are expressed as fold-expression in relation to the nontreated control (40). Gene-specific primers were as follows: HPRT: 5′-CCAGT CAACAAG-3′ and 5′-CACAATCAAGAC-3′; HO-1: 5′-AG GGTGATAGAAGAGGCCAAGACT-3′ and 5′-TTCCACCG-GACAAAGTTCATGGC-3′; TFR1: 5′-TAAACCTGCTGTTGG GGTTC-3′ and 5′-TGCAGGTCTGACAGGTTCTG-3′; ATF3: 5′-CAAGTGCATCTTTGCCTCAA-3′ and 5′-CCACCCGAG GTACAGACACT-3′; and GDF15: 5′-CTCCAGATTCCGAG AGTTGC-3′ and 5′-AGAGATACGCAGGTGCAGGT-3′

Gene-array experiments

Gene-expression profiling was performed by competitive dual-color hybridization of complementary RNA probes on human 4×44 K oligonucleotide microarray chips (Agilent Technologies, Palo Alto, CA), as described (37). To verify integrity, each RNA sample was analyzed on an RNA 6000 Nanochip (Bioanalyzer 2100 instrument, Agilent Technologies, Basel, Switzerland). High-quality total RNA typically had an 18/28S ribosomal RNA ratio >1.5. cRNA probes were synthesized from 200-ng aliquots of high-quality total

RNA by using the low-input fluorescence linear amplification kit protocol and spiked with control targets (Agilent Technologies). Cyanine-3-dCTP (control) or cyanine-5-dCTP (treatment) labeled cRNA probes were purified on RNAeasy mini spin columns (Qiagen) and quantified by spectrophotometer (NanoDrop Technologies, Wilmington, DE). Equal quantities of Cy3- and Cy5-labeled probes (825 μg each) were mixed and incubated in fragmentation buffer in the dark for 30 min at 60°C. After fragmentation control and respective treatment, samples were hybridized on the whole human genome (4×44 K) oligonucleotide microarrays (Agilent Technologies) for 17 h at 60°C in the dark, rotating at 10 rpm. After washing twice in GE wash buffer for 1 min, the microarray slides were washed in acetonitrile and dried. Slides were scanned by using a dual-laser microarray scanner and analyzed with Feature Extraction software (Agilent Technologies) and the Rosetta Resolver 7.2 Gene Expression Data Analysis System (Rosetta Biosoftware, Seattle, WA). All gene-array data have been submitted to www.ebi.ac.uk/arrayexpress and can be accessed through the following reviewer login: *Username: Reviewer_E-MEXP-2263 Password: 1248259780826 Password: 1248259780826.*

iTRAQ labeling and laser-desorption–matrix-assisted laser desorption ionization mass spectrometry

Ferrous Hb was incubated with different GOX concentrations (1.2, 5, and 10 mU/ml) in cell-culture medium containing 4 mg/ml glucose and 5% FCS for 8 h. A total of 30 μg protein of each sample was dried in a speed vacuum concentrator for 3 h and resuspended with 20 μl of dissolution buffer (0.5 M triethylammonium bicarbonate and 0.05% SDS), reduced, and alkylated as described in the iTRAQ protocol (Applied Biosystems, Inc., Foster City, CA). Each sample was digested with 1 mg/ml trypsin (Promega, Madison, WI) at a trypsin-to-protein ratio of 1:10 at 37°C overnight and labeled with the iTRAQ reagent, as described in the manufacturer's manual (Applied Biosystems). The proteins from the control condition were labeled with iTRAQ reagent 114, and oxidized conditions, with 115, 116, and 117, respectively. The labeled samples were pooled and purified by using a cation-exchange cartridge (ICAT; Applied Biosystems). The bound peptides were collected with 10 mM KH$_2$PO$_4$, 350 mM KCl, 25% ACN. The labeled samples were dried in a vacuum concentrator. Dried peptides were redissolved in 20 μl of 2% (vol/vol) acetonitrile/0.1% trifluoroacetic acid, automatically injected by a Famos autosampler and separated by an UltiMate capillary LC system (Dionex - LC Packings) by using a 75-μm ID reverse-phase column.

Nano-LC separation and MALDI target spotting of tryptic peptides. Peptide separation was performed on an Ultimate chromatography system (Dionex-LC Packings, Sunnyvale, CA) equipped with a Probot MALDI spotting device. Five microliters of the samples was injected by using a Famos autosampler (Dionex-LC Packings) and loaded directly onto a 75 μm×150 mm reversed-phase column (PepMap 100, 3 μm; Dionex-LC Packings). Peptides were eluted at a flow rate of 300 nl/min by using the following gradient: 0–10 min, no solvent B; 10–105 min, none to 50% solvent B; and 105–115 min, 50 to 100% solvent B. Solvent A contained 0.1% TFA

in 95:5 water/acetonitrile, and solvent B contained 0.1% TFA in 20:80 water/acetonitrile. For MALDI analysis, the column effluent was directly mixed with MALDI matrix (3 mg/m; α-cyano-4-hydroxycinnamic acid in 70% acetonitrile/0.1% TFA) at a flow rate of 1.1 μl/min via a μ-Tee fitting. Fractions were automatically deposited every 10 s onto a MALDI target plate (Applied Biosystems/MDS Sciex, Foster City, CA) by using a Probot microfraction collector. In total, 416 spots were collected from each HPLC run.

MALDI-TOF/TOF mass spectrometry. MALDI plates were analyzed on a 4800 MALDI TOF/TOF system (Applied Biosystems) equipped with an Nd:YAG laser operating at 200 Hz. All mass spectra were recorded in positive reflector mode and generated by accumulating data from 600 laser shots. First, MS spectra were recorded from peptide standards on each of the six calibration spots, and the default calibration parameters were updated. Second, MS spectra were recorded for all sample spots on the MALDI target plate (416 spots per sample, four samples per plate). The MS spectra were recalibrated internally based on the ion signal of neurotensin peptide (Sigma).

The following threshold criteria and settings were used for the acquisition of MS/MS spectra: mass range, 800 to 4,000 Da; minimum signal-to-noise (S/N) for MS/MS acquisition, 100; maximum number of peaks/spot, eight. Peptide CID was performed at a collision energy of 1 kV and a collision gas pressure of approximately 2.5×10^{-6} Torr. During MS/MS data acquisition, a method with a stop condition was used. In this method, a minimum of 1,000 shots (20 subspectra accumulated from 50 laser shots each) and a maximum of 2,000 shots (40 subspectra) were allowed for each spectrum. The accumulation of additional laser shots was halted whenever at least six ion signals with an S/N of at least 60 were present in the accumulated MS/MS spectrum, in the region above m/z 200.

Peptide and protein identification and quantification by database searching. MS/MS data analysis was performed by using ProteinPilot 2.0.1 software (Applied Biosystems) with the Paragon algorithm as the default search program. Trypsin was selected as the digestion agent, and 4-plex iTRAQ labeling and MMTS modification of cysteine were specified.

Scanning electron microscopy

Cells were cultured on round (12-mm) coverslips. After treatment with GOX (5 mU) and Hb (1 mg/ml) for 8 h, cells were washed and fixed with 2% glutaraldehyde in PBS. The fixed cells were washed and postfixed in 1% OsO₄, dehydrated by successive immersions in increasing concentrations of ethanol, followed by CPD (critical point drying, BaL-TEC CPD 030). The dried coverslips with the dehydrated cells were mounted on SEM carbon stubs and coated with platin (5 nm). Pictures were taken at 2 kV with a SEM Zeiss Gemini 1530 (Zeiss, Oberkochen, Germany).

Statistical analysis

Differences between treatment groups were analyzed with ANOVA and the Bonferroni posttest by using GraphPad Prism version 5.01, where applicable. A *p* value < 0.01 was considered significant.

Results

Reaction with Hb abolishes the accumulation of H_2O_2 generated by the glucose-glucose oxidase (GOX) system in cell culture

To investigate the chemical interactions of low levels of H_2O_2 with extracellular Hb and their influence on cell-viability and gene-expression patterns, we established a glucose-glucose oxidase (GOX) system. This enzymatic system mimics a continuous, and thus, a more physiologic low-level H_2O_2 exposure than does the bolus addition of H_2O_2 (14). The GOX activity of 10 mU/ml in the presence of 4 mg/ml glucose was found to be reproducibly depleting GSH and significantly reducing cell viability over an incubation period of 8 h in VSMCs and in the mouse macrophage cell line RAW264.7. With the luminescent probe AcriglGlow, which emits light in the presence of H_2O_2, we could follow the production and accumulation of H_2O_2 in cell-culture medium, reaching a plateau intensity after an incubation period of 4 h (Fig. 1A). In the presence of Hb, we could not detect any signal over the whole 8-h reaction period. This indicates that either the generation of H_2O_2 is impaired by Hb or that the GOX-generated H_2O_2 is immediately consumed by the peroxidase activity of Hb. The same pattern of GOX-generated H_2O_2 accumulation in cell-culture supernatant and complete depletion of H_2O_2 by Hb could be confirmed by using an alternative assay based on AmplexRed fluorescence (Fig. 1B). The presence of Hb did not affect the performance of the H_2O_2 assays, as comparable results were obtained when samples were ultrafiltrated (to remove Hb) before measurements.

The reactions of Hb heme-iron with GOX-derived H_2O_2 were studied with spectrophotometry. Previous work by Cashon and Alayash (9) demonstrated differences in ferrous Hb and chemically cross-linked Hbs in their ability to form stable ferryl Hb. UV-visible spectrophotometry data consistent with Cashon and Alayash shows that ferrous Hb briefly engages in a pseudoperoxidase reaction in the presence of H_2O_2 generated by the glucose/GOX system (Fig. 1B, left). However, when starting with ferrous Hb, the peroxidase activity is lost within 50 min after the start of the reaction, and both heme and Hb become degraded in the spectra. Conversely, when ferric Hb is exposed to the same glucose/GOX system of H_2O_2 generating the ferric, heme spectra remains stable over >2 h of continuous H_2O_2 exposure (Fig. 1C right). For the starting material ferrous Hb, the concentration changes of ferric and ferryl Hb with the loss of ferrous Hb are shown in Fig. 1D, E. UV-VIS spectrophotometry revealed a time-dependent oxidation of heme iron in the presence of GOX, and therefore proves that Hb-heme reacts with the GOX-generated H_2O_2. Thus, the absence of H_2O_2 accumulation in the presence of Hb is not a result of suppressed enzymatic activity or the decomposition of H_2O_2 by possible Hb contaminants such as superoxide dismutase and catalase. Instead, GOX-generated H_2O_2 is consumed by Hb. Importantly, in all these studies, we used a highly purified and extensively characterized Hb preparation that has been proven to contain no RBC superoxide dismutase or catalase contamination.

FIG. 1. Heme redox-cycle and consumption of GOX-derived H_2O_2 by Hb. (A) H_2O_2 accumulation in the cell-culture medium resulting from an active glucose-GOX system (4 mg/ml glucose, 10 mU/ml GOX) was intermittently measured with the H_2O_2-induced luminescence of AcriGlow (first measurement, ~15 min after the start of reaction). No H_2O_2 could be detected when Hb at 1 mg/ml was added at the beginning of the reaction (*black dots*). (B) Alternatively, H_2O_2 generated by GOX was measured in VSMC cell-culture supernatants with the Amplex Ultra Red assay after incubation with or without Hb for 8 h. Ultrafiltration at the end of the incubation/reaction period to remove Hb from the sample medium did not change assay results. (C) Damaged hemoglobin is observed in the 500- and 700-nm regions of the UV-visible spectra when the starting material is ferrous Hb (*left*) compared with ferric Hb (*right*). In culture media with fetal calf serum, spectra were obtained every 2 min over a 2-h period and demonstrated a gradual increase in absorbance at these wavelengths, starting at 50 min after the addition of GOX to ferrous Hb. Conversely, ferric Hb remained stable in the HbFe^{3+} form over a 2-h period. (D) Addition of 2 mM sodium sulfide (Na$_2$S) generates the spectra for sulf-Hb (a measure of ferryl Hb; *dotted line*). (E) The time course of ferrous (Fe^{2+}), ferric (Fe^{3+}), and ferryl (Fe^{4+}) Hb is shown before Hb damage and determined as described in Materials and Methods. In all panels, data from one representative experiment are shown.
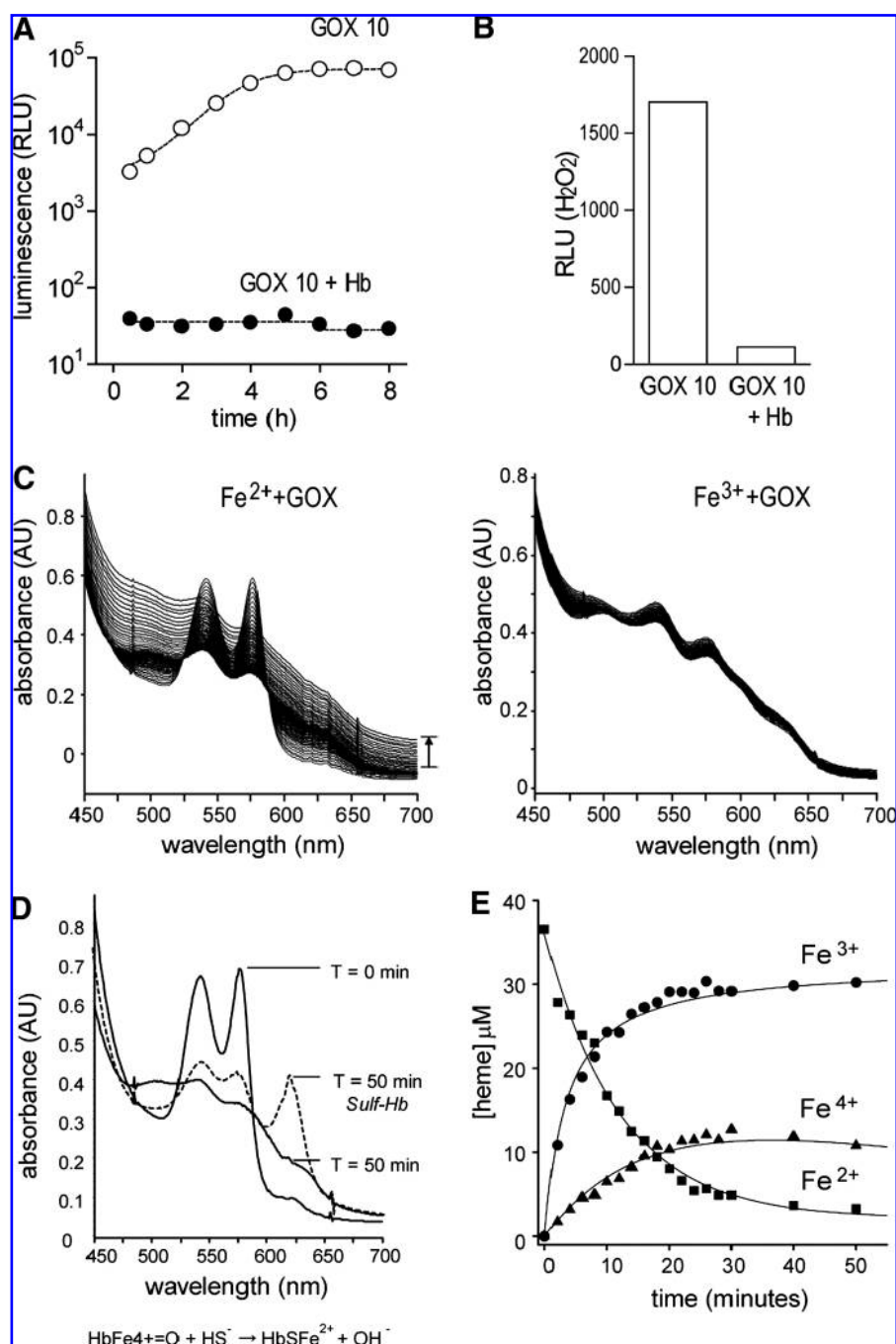
Screening of cell spreading and cell viability by impedance measurement suggests a protective role of ferrous and ferric Hb against H_2O_2-mediated oxidative cell damage

We measured cell monolayer impedance of HEK293 cells as a function of time in the presence of different concentrations of glucose oxidase and with or without 3 mg/ml of either ferrous or ferric Hb. The xCELLigence system used in these studies provides a cell index (CI) that increases as a function of cell attachment, spreading, and cell growth, and, conversely, declines as a function of cell detachment and cell death.

In Fig. 2A, the homogeneous attachment and spreading of HEK293 cells in culture (in a 96-well plate) is shown. Figure 2B illustrates the cellular (CI) response to different GOX-generated H_2O_2 levels. Different concentrations of GOX with and without Hb (Fe^{2+} or Fe^{3+}) were added to the cell culture 4 h after seeding (indicated by the black arrows). A dose- and time-dependent decrease in CI could be observed with GOX in the absence of Hb. The drastic decline in CI observed with 10 mU/ml and 5 mU/ml of GOX was associated with visible rounding of the cells and detachment after >20 h of incubation. In contrast, the still significant but slighter changes in CI observed at 2.5 mU/ml GOX that
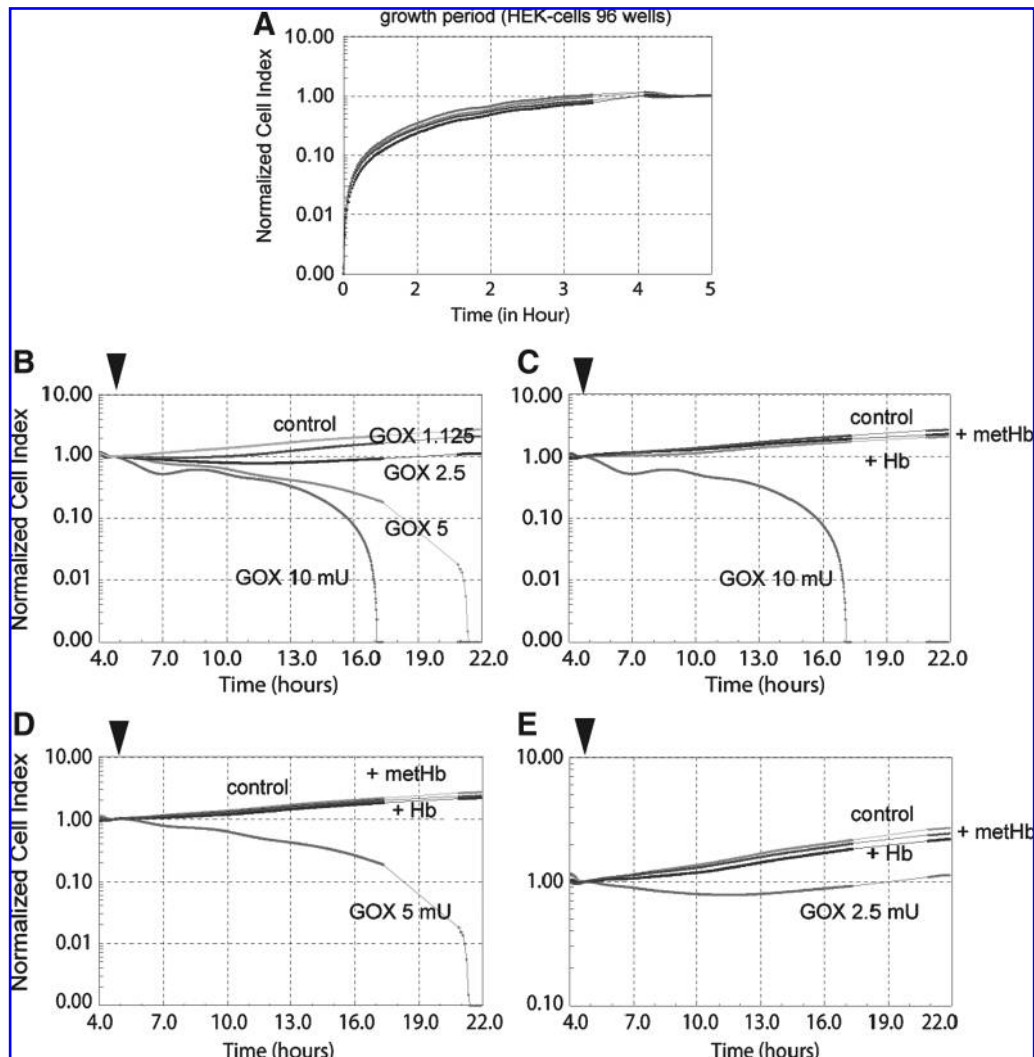
FIG. 2. On-line cell-culture impedance measurement: cell spreading, growth, and H_2O_2 toxicity. Impedance was measured on-line in cell culture by using the CELLligence RTCP-SP system. HEK293 cells were seeded at time 0 min, and the cell index, which is a function of adherence, spreading, and cell growth, was measured every 5 min (**A**). After 4 h, growth medium was replaced with serum-free medium containing the indicated concentrations of glucose oxidase (GOX) with or without Hb (as Fe^{2+} or Fe^{3+}). The cells were kept in culture for another 18 h (**B–E**). The decline of the cell index observed in the presence of the higher GOX concentrations was associated with extensive rounding of the cells, subsequent detachment from the cell-culture surface, and cell death. No morphologic changes were observed in the presence of Hb. Individual data points represent the mean of independent values from eight wells acquired every 5 min. (For interpretation of the references to color in this figure legend, the reader is referred to the web version of this article at www.liebertonline.com/ars).

produce steady-state H_2O_2 concentrations far less than $10 \mu M$ did not result in visible changes in cell morphology. Cell-impedance measurement thus proved to be a sensitive method to detect H_2O_2-induced cellular responses in real time. As shown in Fig. 2C–E, ferrous and ferric Hb completely prevented the H_2O_2-induced changes in CI. Similar experiments were performed with incubation times and on-line monitoring of up to 40 h. No difference between control and GOX + Hb samples could be detected at any time-point and H_2O_2-exposure level tested.

After having demonstrated that both ferric and ferrous Hb can protect against H_2O_2-mediated cell damage, we performed the following studies with ferrous Hb, because we considered exposure to ferrous or mixed ferrous/ferric Hb a more physiologic condition than exposure to exclusively ferric Hb.

Decomposition by ferrous Hb prevents cellular GSH depletion and cell death during H_2O_2-mediated oxidative stress

The oxidative stress exerted by H_2O_2 exposure depletes cellular antioxidant systems, such as reduced GSH, and eventually induces cell death by apoptosis or necrosis. To confirm and interpret the real-time results obtained with impedance measurement, we measured intracellular GSH and ATP as quantitative markers of cellular antioxidant capacity and cell viability, respectively, in the absence and in the presence of different concentrations of GOX. We also examined different and physiologically more relevant cell types (macrophages and vascular smooth muscle cells) than in the screening experiments. After 8 h, we found a dose-dependent depletion of GSH and ATP, which resulted in an almost 100%

FIG. 3. Hb prevents glutathione and ATP depletion in vascular smooth muscle cells and macrophage-like cells exposed to GOX-generated H_2O_2. Intracellular-reduced glutathione (GSH) and ATP levels were measured as surrogate markers for cellular antioxidant capacity and viability, respectively, after 8 h of exposure to H_2O_2 generated by different GOX concentrations/activities (1.2–80 mU/ml). In the presence of Hb (1 mg/ml, red dots), the GOX activity-dependent decline curves for GSH and ATP are significantly shifted toward the right, indicating a protective effect of Hb on cellular redox status and viability. Luminescence is shown relative to that of nontreated cells. Data represent mean ± SD of at least three independent experiments. Differences of treatment groups were statistically analyzed with ANOVA for GOX, 10 mU/ml, and GOX, 20 mU/ml, and were found to be significantly different (*$p < 0.001$).
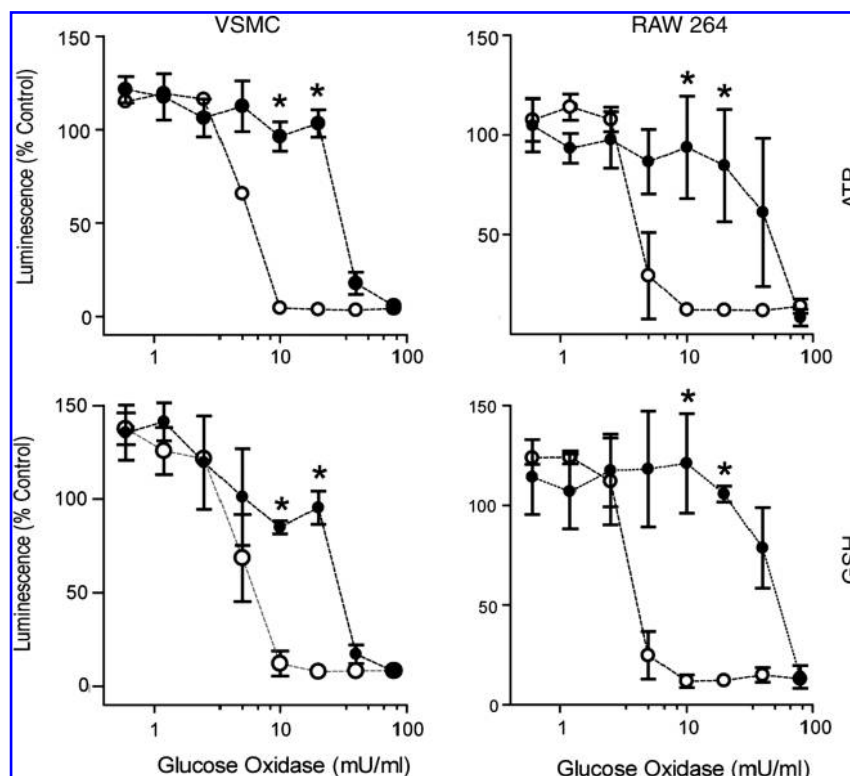
loss of GSH and ATP at concentrations of more than 5 mU/ml GOX (Fig. 3). This observation was compatible with the light-microscopy observation of extensive cell detachment after >12-h exposure to GOX activities above 10 mU/ml. Both intracellular GSH and ATP levels were maintained at baseline levels up to GOX activities of 20 mU/ml when Hb, at a concentration of 1 mg/ml, was added to the cell culture. After establishing that Hb can prevent H_2O_2-induced GSH and intracellular ATP depletion, we aimed to confirm on a transcriptional level that Hb also can prevent the cellular transcriptional stress response induced on H_2O_2 exposure.

Hb blunts the H_2O_2-driven oxidative stress transcriptional response in vascular smooth muscle cells

To assess the global transcriptional response to H_2O_2 exposure generated by the GOX system, we have compared the RNA expression profile of VSMCs exposed to 5 mU/ml of GOX for 8 h in the absence or presence of 1 mg/ml Hb. The activity of 5 mU/ml of GOX was reproducibly associated with a measurable reduction in cellular GSH and ATP levels, but did not result in visible cytotoxicity within the 8-h incubation period. The global gene-expression pattern induced by GOX ± Hb, as assessed by the relative abundance of >19,000 Unigene clusters, represented on the Agilent human whole-genome arrays is shown in Fig. 4. In this representation of the transcriptome data, it becomes evident that the H_2O_2 exposure induces a vivid change of gene expression with many up- or downregulated genes, as indicated by the wide spreading of gene data points along the (log) ratio axis (y-axis in Fig. 4), which indicates the ratio of RNA abundance of treated compared with untreated VSMCs. Compatible with

the previously described consumption of GOX-generated H_2O_2 by Hb, the spread of gene-expression data is significantly reduced when Hb is present in the system. In GOX-treated cells, we found 2,157 genes upregulated and 2,386 genes significantly ($p < 0.01$) downregulated. Of these, 711 were regulated more than threefold. In contrast, in the cells coincubated with GOX and Hb, we found only 1,530 and 969 genes significantly up- or downregulated, respectively, with only 108 genes regulated at a ratio above threefold (Fig. 5A). The influence of Hb on individual gene-expression levels is illustrated in Fig. 5B, in which the pairwise representation of highly H_2O_2-induced transcripts in the presence and absence of Hb highlights the activity of Hb to suppress H_2O_2-driven gene expression. High ratios of gene induction by GOX-generated H_2O_2 were observed for activating transcription factor 3 (ATF3) and growth-differentiation factor 15 (GDF15). ATF3 is a well-characterized oxidative stress response transcription factor; GDF15 is a stress-inducible member of the transforming growth factor superfamily. We confirmed by quantitative RT-PCR that ATF3 and GDF15 are highly induced by GOX-generated H_2O_2 and that this oxidative stress response is completely suppressed when Hb (1 mg/ml) is added to 10 mU/ml of GOX (Fig. 6). That H_2O_2 is involved in the GOX-driven alteration in gene expression in our experiments is confirmed by the fact that catalase also completely abrogates the GOX-induced ATF3 response (Fig. 6B). A similar differential gene-expression response was found for the inflammation-associated transcripts CXCL-4 and COX2. Although Hb generally reduces H_2O_2-stimulated alteration in gene expression in our cell-culture system, the reaction of H_2O_2 with Hb enhances the H_2O_2-induced expression of the antioxidant heme-breakdown enzyme heme oxygenase (HO-1). This response is likely to be mediated by enhanced heme
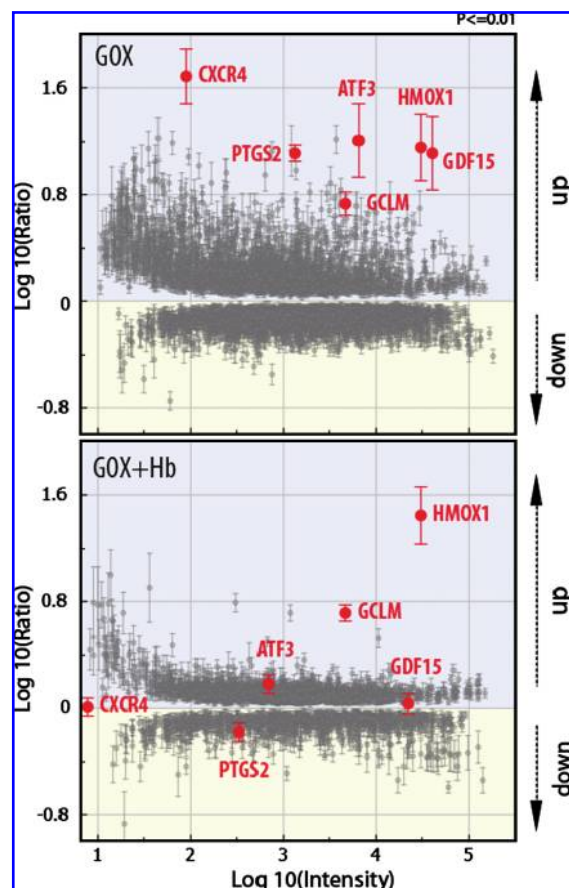
FIG. 4. **Oligonucleotide gene-array analysis of vascular smooth muscle cell gene expression evoked by GOX-generated H_2O_2 in the absence or presence of Hb.** Human VSMCs were exposed to the weakly cytotoxic activity of GOX (5 mU/ml) in the absence (*upper panel*) or in the presence (*lower panel*) of 1 mg/ml Hb for 8 h. The global transcriptome profile of three independent experiments was then determined with competitive hybridization gene-array analysis (Agilent human whole genome 4×44 K arrays). Each numeric result of an individual data point represents the ratio of the expression level of one gene in treated cells *versus* nontreated (control) cells. The expression levels of different sequences on the array that represent the same Unigene cluster were combined by using the Rosetta Resolver in-built error algorithm to combine experimental data on a Unigene level. Each dot represents the mean (±error of three experiments) of the expression ratio of one individual Unigene cluster (gene). Only genes with an mRNA expression ratio significantly different from 1 ($p < 0.01$) are shown. Upregulated genes (log ratio >0) are within the blue area, and downregulated genes (log ratio <0) are within the yellow area of the plot. The X-axis represents the hybridization signal intensity that is roughly proportional to the baseline mRNA abundance. (The gene symbols highlighted in red are *ATF3*, activating transcription factor 3; *GDF15*, growth-differentiation factor 15; *HMOX*, heme oxygenase 1; *GCLM*, glutamate-cysteine ligase modifier subunit; *CXCR4*, chemokine (CXC motif) receptor 4; *PTGS2*, prostaglandin-endoperoxide synthase 2 (COX2). For exact fold changes and *p* values of individual genes, see Table 1. (For interpretation of the references to color in this figure legend, the reader is referred to the web version of this article at www.liebertonline.com/ars).

release from oxidized Hb (Fig. 6D). The latter hypothesis is supported by the observation that when heme release from methemoglobin is inhibited by the addition of stoichiometric concentrations of the Hb-binding plasma protein, haptoglobin (Hp), the superinduction of HO-1 can be suppressed (data not shown). We recently showed that complex formation with Hp does not alter the ability of Hb to redox cycle H_2O_2 (7).

Extensive Hb amino acid oxidation and precipitation suggests that globin acts as a scavenger for heme-generated radicals in the presence of GOX-generated H_2O_2

Under highly controlled reaction conditions (*i.e.*, bolus addition of a 10-fold molar concentration of H_2O_2 to Hb in the absence of small molecular reductants or other proteins or both), the reaction of H_2O_2 with Hb results in a reproducible pattern of β-globin chain amino acid oxidations and α-globin chain polymerization. Primary oxidized amino acids within the Hb β-chain are Cys93, Trp15, and Cs112. These cross-linking and amino acid oxidation reactions are supposed to be driven by the radicals generated in the reaction of Hb-heme with H_2O_2. Therefore, the protective activity of Hb against H_2O_2-induced oxidative stress in our cell-culture systems could be a combined result of H_2O_2 removal by heme redox cycling and subsequent scavenging of toxic radicals within Hb cross-links and globin amino acid oxidations. To find the structural evidence of these events, we applied a quantitative mass-spectrometry method on the basis of isobaric tag peptide labeling (iTRAQ) in combination with MALDI-TOF-MS/MS to measure the extent of GOX-driven oxidation of βCys93. As shown in Fig. 7, the presence of GOX at 5 or 10 mU/ml shifts the ratio of oxidized to nonoxidized cysteine toward a >20-fold excess of triply oxidized cysteic acid over the nonoxidized globin after an 8-h incubation period. In addition, the H_2O_2 reaction with Hb in our cell-culture conditions results in a dense precipitate. This precipitate, which did not occur at all when cells were incubated with any concentration of only Hb or GOX, probably corresponds to the heme-adducted globin polymers, which we previously characterized by high-mass MALDI MS (Fig. 8).

Discussion

The radicals emanating from Hb when it reacts with oxidants have been proposed to be a primary source of Hb-derived toxicity (8, 10). Conversely, the reaction of Hb with hydrogen peroxide can potentially remove the potentially toxic oxidant from peroxidative environments. Multiple kinetic and environmental factors might therefore determine the net biologic effect of radical generation and H_2O_2 removal by Hb during oxidative-stress conditions. In this study, we showed that ferrous and ferric Hb can protect various cell types against the cytotoxicity that normally results from the continuous low-level H_2O_2 exposure generated by an enzymatic system. Additionally, the transcriptional stress response exerted by this low-level H_2O_2 exposure was effectively suppressed by Hb, thus supporting a true antioxidant potential of Hb. The rationale used to explain the H_2O_2 consumption and associated cellular protection observed in our systems is demonstrated in the UV-visible spectra, where ferrous and ferric Hb are shown to redox cycle H_2O_2 generated by the GOX enzymatic system in cell-culture conditions.

TABLE 1. TRANSCRIPTS MORE THAN FIVEFOLD INDUCED BY GOX TREATMENT OF VSMCs
FOR 8 h AND CORRESPONDING DATA FOR GOX TREATMENT IN THE PRESENCE OF FERROUS HB

| UniGene code		Description	GOX (n = 3)		GOX + Hb (n = 3)	
			Fold change	p Value	Fold change	p Value
Hs.421986	**CXCR4**	**Chemokine (C-X-C motif) receptor 4**	**47.638**	**1.14E-22**	**1.005**	**0.937**
Hs.530749	PPFIA4	Protein tyrosine phosphatase	16.277	2.40E-17	1	1
Hs.9613	ANGPTL4	Angiopoietin-like 4	16.062	2.29E-40	−1.267	0.002
Hs.460	**ATF3**	**Activating transcription factor 3**	**15.84**	**5.79E-07**	**1.477**	**5.4E-08**
Hs.517581	**HMOX1**	**Heme oxygenase (decycling) 1**	**14.042**	**4.28E-08**	**27.373**	**1.4E-15**
Hs.47357	CH25H	Cholesterol 25-hydroxylase	13.587	5.15E-22	1.052	0.888
Hs.530443	LOC387763	Hypothetical LOC387763	13.176	2.18E-10	1.052	0.689
Hs.25647	FOS	V-fos FBJ murine osteosarcoma viral	13.138	0	1.023	0.7
Hs.196384	**PTGS2**	**Prostaglandin-endoperoxide synthase**	**12.637**	**0**	**−1.536**	**4.3E-12**
Hs.515258	**GDF15**	**Growth-differentiation factor 15**	**12.561**	**2.82E-06**	**1.061**	**0.457**
Hs.172130	ZP1	Zona pellucida glycoprotein 1	12.005	0	−2.028	0.241
Hs.159523	CRTAM	Class-I MHC-restricted T-cell associated	11.483	0	1	1
Hs.268490	NR0B1	Nuclear receptor subfamily 0, group B	11.046	5.75E-21	2.438	2.5E-05
Hs.413297	RGS16	Regulator of G-protein signaling 16	10.196	2.46E-32	−1.197	0.176
Hs.9730	TAC3	Tachykinin 3 (neuromedin K, neurokinin	9.812	2.63E-24	1	1
Hs.390594	SLC7A11	Solute carrier family 7, member 11	9.453	0	5.098	0
Hs.492490	PVRL4	Poliovirus receptor related 4	9.452	4.93E-08	1	1
Hs.83465	HOXD1	Homeobox D1	9.206	8.13E-22	1.298	0.56
Hs.642679	MAFB	V-maf musculoaponeurotic fibrosarcoma	9.107	2.57E-24	−1.03	0.766
Hs.611485	Hs.611485	*Homo sapiens*, clone IMAGE:2960704	8.04	4.24E-08	1.749	0.098
Hs.583896	C8orf12	L-threonine dehydrogenase	7.97	1.08E-10	1	1
Hs.390221	TEX14	Testis-expressed sequence 14	7.914	1.61E-11	1.065	0.722
Hs.288998	S100A14	S100 calcium-binding protein A14	7.868	9.53E-13	−1.124	0.808
Hs.534313	EGR3	Early growth response 3	7.639	3.69E-11	1	1
Hs.96	PMAIP1	Phorbol-12-myristate-13-acetate induced	7.582	7.07E-16	1.253	1.8E-04
Hs.631555	DHDH	Dihydrodiol dehydrogenase (dimeric)	7.581	0	−1.115	0.586
Hs.592601	AK3L1	Adenylate kinase 3–like 1	7.567	3.04E-10	1.217	0.167
Hs.17958	GAL3ST1	Galactose-3-O-sulfotransferase 1	7.364	1.78E-29	2.8	1.6E-04
Hs.584876	FLRT1	Fibronectin leucine-rich transmembrane	7.021	7.66E-07	1.127	0.767
Hs.150595	CYP26A1	Cytochrome P450, family 26, subfamily A	6.957	6.19E-09	−1.007	0.985
Hs.264606	Hs.264606	Full-length insert cDNA clone ZD68B12	6.955	4.52E-21	1.27	0.328
Hs.181297	LOC283666	Hypothetical protein LOC283666	6.944	2.26E-05	1.094	0.294
Hs.632832	RAB39B	RAB39B, member RAS oncogene family	6.83	1.45E-14	−1.082	0.577
Hs.48029	SNAI1	Snail homologue 1 (*Drosophila*)	6.676	4.66E-29	1.103	0.237
Hs.594689	Hs.594689	Full-length insert cDNA clone ZE05E03	6.661	3.76E-16	2.65	0.002
Hs.519162	BTG2	BTG family, member 2	6.42	0	−1.058	0.429
Hs.349204	SOST	Sclerosteosis	6.418	7.90E-08	1	1
Hs.231897	FLJ35767	FLJ35767 protein	6.391	1.82E-14	2.076	0.024
Hs.132701	CCDC11	Coiled-coil domain containing 11	6.379	3.45E-08	2.156	0.228
Hs.1027	RRAD	Ras-related associated with diabetes	6.326	0	−1.096	0.097
Hs.420244	FAM80A	Family with sequence similarity 80	6.275	6.61E-20	1.132	0.756
Hs.2233	CSF3	Colony-stimulating factor 3 (granulocyte)	6.272	0	−1.485	0.215
Hs.563344	NR4A2	Nuclear-receptor subfamily 4, group A	6.259	7.10E-14	1.221	0.354
Hs.469663	ZSCAN4	Zinc-finger and SCAN domain–containing 4	6.239	3.02E-25	1.525	0.322
Hs.636352	Hs.636352	CDNA: FLJ23572 fis, clone LNG12403	6.076	7.94E-05	−1.018	0.958
Hs.444947	TRIB1	Tribbles homologue 1 (*Drosophila*)	6.009	4.14E-29	1.324	0.02
Hs.539969	ARHGAP9	Rho GTPase–activating protein 9	5.839	1.05E-10	−1.063	0.849
Hs.437126	SPATA4	Spermatogenesis-associated 4	5.832	0	1.085	0.644
Hs.481235	ACTA1	Actin, alpha 1, skeletal muscle	5.759	3.54E-14	2.08	0.155
Hs.1288	ARC	Activity-regulated cytoskeleton-associated	5.646	0	−1.198	0.324
Hs.40888	AOC3	Amine oxidase, copper-containing 3	5.603	1.45E-07	1.312	0.026
Hs.198241	JMJD1A	Jumonji domain–containing 1A	5.57	0	1.359	1.0E-06
Hs.557425	GDF9	Growth-differentiation factor 9	5.565	3.06E-22	−1.056	0.895
Hs.25022	RASL11B	RAS-like, family 11, member B	5.45	2.08E-14	−1.306	0.067
Hs.8035	AREG	Amphiregulin	5.42	1.80E-42	1.634	0.001
Hs.270833	**GCLM**	**Glutamate-cysteine ligase**	**5.288**	**0**	**5.104**	**0**
Hs.315562	GRHL3	Grainyhead-like 3 (*Drosophila*)	5.263	5.09E-19	1.207	0.609
Hs.369825	TRIM73	Tripartite motif–containing 73	5.214	7.66E-15	1.546	0.106
Hs.632307	FOSB	FBJ murine osteosarcoma viral oncogene	5.165	0	1.255	0.109
Hs.590958	CXCL3	Chemokine (C-X-C motif) ligand 3	5.151	9.40E-22	−1.124	0.026
Hs.89690	FLJ26850	FLJ26850 protein	5.083	2.21E-09	1.251	0.646
Hs.628968	SPANXB2	SPANX family, member B2	5.069	5.55E-06	−1.104	0.368
Hs.643547	HK2	Hexokinase 2	5.056	4.13E-15	1.029	0.741
Hs.591588	Hs.437039	CDNA clone IMAGE:5288757	5.05	3.04E-05	1.813	0.242
Hs.437039	LOC644242	Hypothetical protein LOC644242	5.028	2.31E-08	1.647	0.372
Hs.515383	MGC42105	Hypothetical protein MGC42105	5.003	2.03E-32	−1.136	0.453

Genes in boldface are highlighted in Fig. 3.
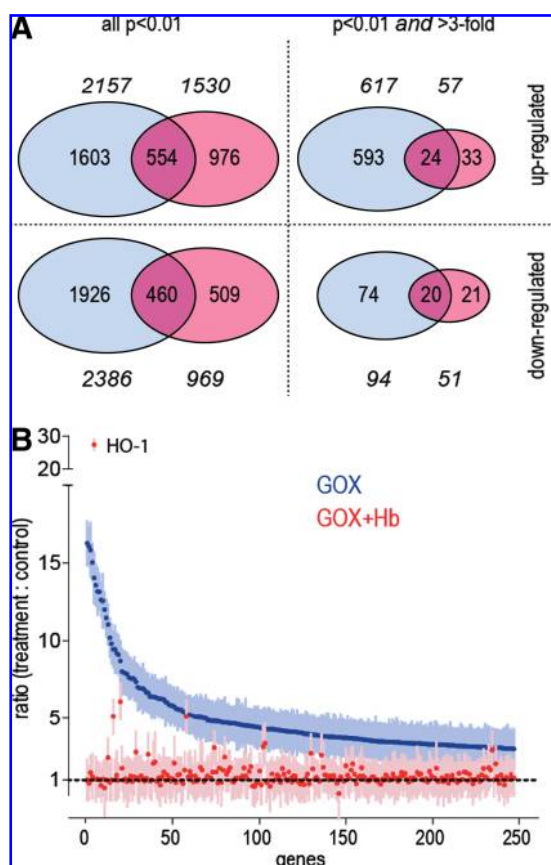
FIG. 5. Summary of transcript regulations found with gene-array analysis of GOX-driven gene expression in the absence or presence of Hb. (A) The Venn diagrams represent total numbers of transcripts found to be significantly ($p < 0.01$) up- or downregulated by GOX (5 mU/ml) in the absence (blue) or presence (red) of 1 mg/ml of Hb. In the left diagrams, all significantly regulated genes are shown; in the right diagrams, only those with a fold induction/suppression of >3 are shown. (B) Significantly regulated genes represented according to their fold regulation found in GOX (5 mU/ml)-treated VSMCs (blue). Regulations of the same genes in the presence of GOX + Hb (1 mg/ml) are shown at the corresponding X-axis positions in red. Data represent mean ratios of treated *versus* nontreated cells of three independent experiments (±error). A ratio of 1 indicates no change in transcript abundance. For exact fold changes and *p* values of individual genes, see Table 1. (For interpretation of the references to color in this figure legend, the reader is referred to the web version of this article at www.liebertonline.com/ars).

As structural consequences of these reactions, we found extensive Hb β-globin amino acid oxidations and formation of altered heme-protein products observed as aggregates with electron microscopy.

Potential *in vivo* substrates found to be highly vulnerable to the redox cycling and associated radical-generating activity of Hb are lipoproteins (LDL) and fatty acids, such as arachidonic acid, that are ubiquitously present in circulation and as critical structural components of cell membranes (26, 27, 36). The oxidation of these biomolecules can result in the generation of biologically active compounds with a wide range of inflammatory and vasoactive properties. Evidence that these Hb-driven reactions do occur *in vivo* has been provided by the
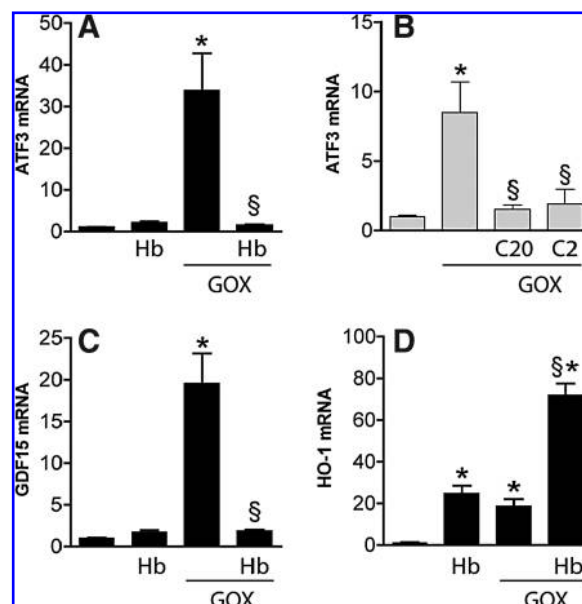

FIG. 6. RT-PCR quantification of oxidative stress–responsive genes in VSMCs. The mRNA abundances of oxidative stress–responsive genes were determined with quantitative RT-PCR after incubation for 8 h with GOX (5 mU/ml) in the presence or absence of 1 mg/ml Hb (A, C, D) or in the presence or absence of catalase at a GOX/catalase activity ratio of 1:2 (C2) or 1:20 (C20) (B). All mRNA levels were normalized to HPRT abundance and are expressed relative to the mRNA abundance in untreated cells. Data represent mean ± SEM of at least three independent experiments. *$p < 0.01$ for differences *vs.* untreated. §$p < 0.01$ for differences in GOX *vs.* GOX + Hb or GOX *vs.* GOX + C.

observation that specific oxidative-stress markers such as 4-hydroxynonenol (4-HNE)-modified proteins are highly increased in tissues when animals are exposed to large quantities of cell-free intravascular Hb (4). *In vitro*, ferric Mb and certain chemically modified Hbs were found to induce cellular oxidative toxicity (12, 13). The toxicity resulting from reaction of heme-proteins with H_2O_2 might be particularly important when small molecular antioxidants, such as ascorbic or uric acid, responsible for physiologically reducing oxidized heme-iron, become depleted either on massive extracellular Hb accumulation or during prolonged oxidative stress (11).

The pseudoperoxidase activity of heme globins (*i.e.*, Hb and myoglobin Mb) was recognized decades ago. Specific heme-pocket amino acid mutations that rapidly remove H_2O_2 generated by autoxidation have been studied (2), and it was thereby suggested that the physiologic environmental exposure of heme globins with enhanced pseudoperoxidase activity could introduce a protective function into the protein. Further work suggested that the stabilization of Hb by chemical modification could enhance the pseudoperoxidative cycling of H_2O_2 by heme, with detrimental consequences to endothelial cells (12). Similar *in vitro* observations were made when cultured endothelial cells were treated with ferric Mb and a constant level of H_2O_2 (13). In light of the potentially hazardous effects exerted by Mb- and modified Hb-derived radicals, the H_2O_2-degrading function of Hb has never been accounted for as an antioxidant or a protective physiologic function of Hb. It appeared likely that, also in the case of
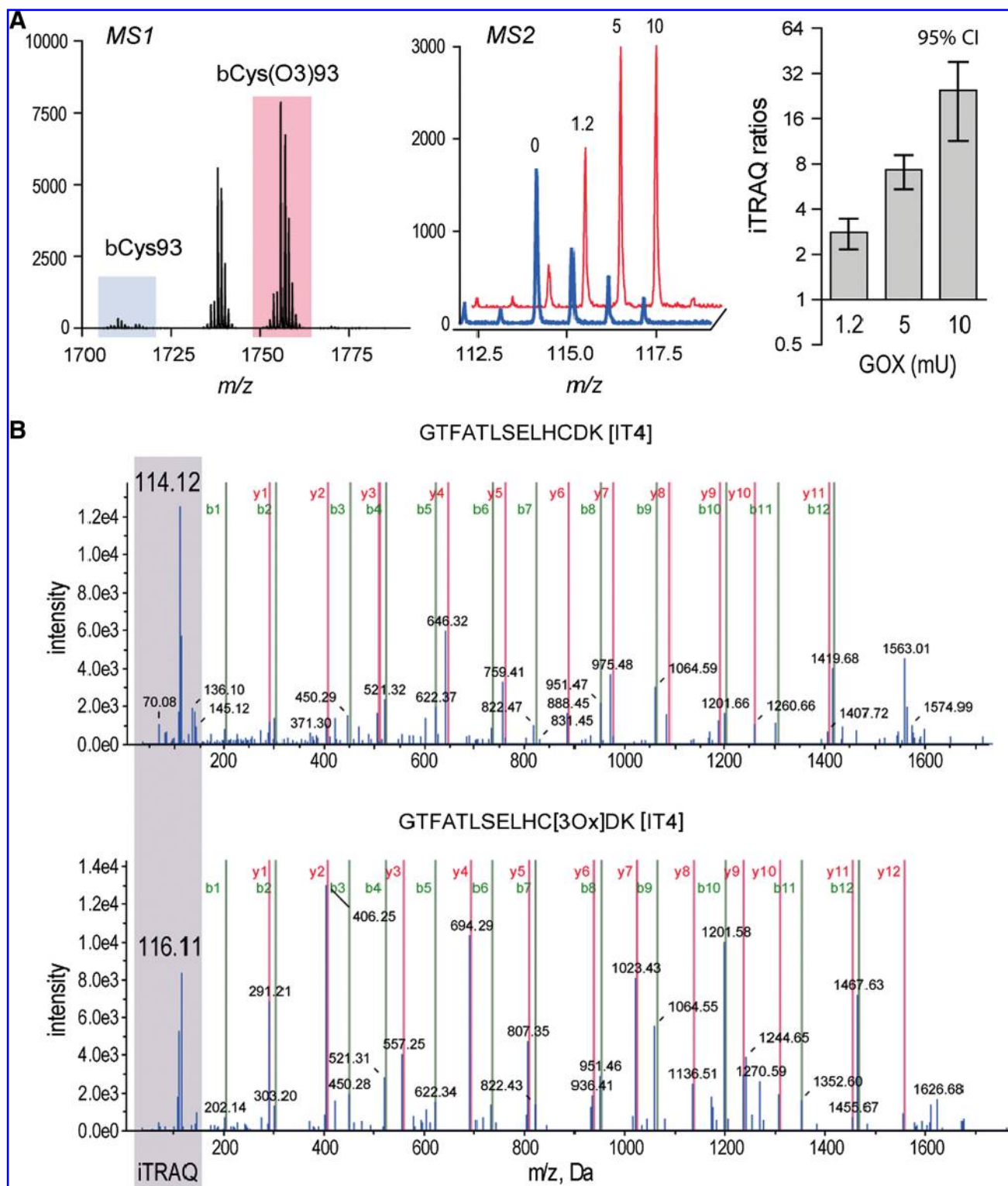
FIG. 7. GOX activity in cell-culture medium induces extensive oxidation of βCys93. Hemoglobin incubated for 8 h with different concentrations of GOX (0–10 mU/ml) in cell-culture medium was analyzed with iTRAQ labeling and MALDI-MS/MS mass spectrometry to quantify nonoxidized and triply oxidized βCys93. (**A**, *left*) Representative ion-current elution profiles of nonoxidized (blue) and oxidized βCys93 in MS1. (**A**, *middle*) Representative MS2 spectra of the iTRAQ tag mass regions for nonoxidized (blue) and oxidized (O_3, red) βCys93. Each of the four individual peaks represents the relative quantity of nonoxidized or oxidized βCys93(O_3) within one sample in the analyte mixture. The analyte mixture was composed of equal amounts of tryptic peptides from Hb treated with the different GOX concentrations, with each sample peptide tagged with a specific iTRAQ mass (114–117 m/z units). (**A**, *right*) The mean cysteic acid (O_3) ratio for treated (three different GOX concentrations) *versus* nontreated Hb is shown as the mean ± 95% confidence interval (CI) of three experiments. The 95% CI for all three GOX conditions does not overlap with the ratio value 1. (**B**) Fragmentation MS2 spectra of the βCys93 containing tryptic peptide GTFATLSELHCDK. Nonoxidized peptide (*upper panel*). Oxidized (O_3) peptide (*lower panel*). (For interpretation of the references to color in this figure legend, the reader is referred to the web version of this article at www.liebertonline.com/ars).
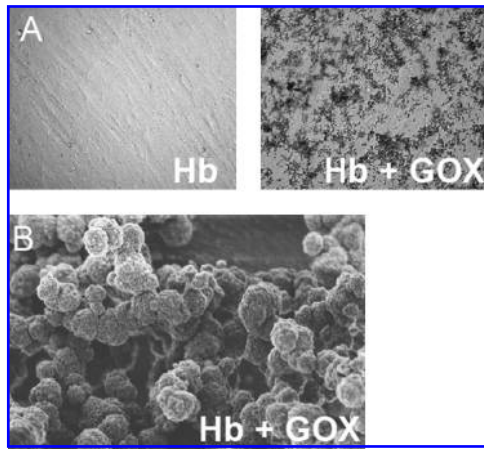
FIG. 8. **Scanning electron microscopy (SEM) image of Hb precipitate forming on VSMC cell culture on reaction of Hb with GOX-derived H_2O_2.** (**A**, *left*) Light microscopy image ($\times 200$ magnification) of a VSMC monolayer in the presence of $1 \, mg/ml$ Hb after 8-h incubation. (**A**, *right*) In the presence of $5 \, mU/ml$ of GOX, a dense precipitate starts to form after $\sim 4 \, h$ of incubation. (**B**) Scanning electron microscope image of the Hb precipitate on VSMC ($\times 40$ magnification, image obtained at $2 \, kV$).

native, nonmodified Hb, radical generation would predominate and skew the net effect of the Hb-H_2O_2 reactions into an oxidant and damaging biologic activity. The present study differs from previous work in that highly purified and stroma-free human Hb preparations were tested to evaluate Hb protein and cellular changes in the presence of a peroxide-generating system. Moreover, our data suggest that differences may exist among the various heme-globin peroxidase activities and their influence on cellular responses.

When Hb is reacted with H_2O_2 at physiologic pH, β-globin chain amino acid structural changes were observed in several studies with different techniques, including HPLC, mass spectrometry, (ESI-TOF/MS), and circular dichroism (21). The most striking modifications were amino acid oxidations within the β-globin chain, a loss of β-globin chain α-helical structure, and decreased ellipticity in the Soret region of the CD spectrum, indicating heme loss of approximately 70% with the addition of stoichiometric concentrations of H_2O_2. Within the α-globin chains, numerous heme/porphyrin Hb protein adducts and cross-links were observed (8, 21, 42).

The intriguing and complex structural changes observed when Hb is subjected to H_2O_2 exposure, and the evident cytoprotective activity of Hb during H_2O_2 exposure, support a novel protective mechanism by which Hb appears to limit cellular injury, contrary to the previously reported data when ferric Mb and certain chemically modified Hbs were evaluated (12). Certain peroxidases (mammalian and plant) exist with heme covalently bound within the active site of the peroxidase enzyme. This structural feature prevents damage to the active site by potentially reactive oxidative products of the peroxide enzymatic degradation (19, 20, 43). Therefore, it is possible that Hb uses a mechanism to protect the external cellular environment by redirecting the radical burden toward heme adduct formation, internalization of heme within the protein, heme cross-linking, or a combination of these. Likewise, a mechanism including irreversible oxidative

modifications of globin amino acids could act as a sink for heme reaction–derived radicals protecting non-Hb substrates and living cells from oxidative impact. At least in the case of ferrous Hb, our spectrophotometric and EM data suggest that these cyclic reactions finally result in complete destruction of the protein.

Under the experimental conditions presented in our study, Hb can act as an antioxidant and cytoprotective peroxidase. A typical clinical situation in which large amounts of extracellular Hb could be exposed to H_2O_2 within an inflammation-prone tissue environment might be found in atherosclerotic plaques. Boyle *et al.* (6) recently reported the intriguing observation that macrophages confined to the regions of intraplaque hemorrhage displayed significantly less oxidative damage as compared with cells within the lipid-core area of the same plaques. Whereas an antioxidative phenotype of the macrophage itself was invoked to explain this unexpected finding, the Hb-rich environment could be an additional protective antioxidant factor.

This concept adds a novel facet to the complex biology of Hb. Our results suggest that the general view of Hb being a toxic and oxidative molecule might be too simplistic. Instead, complex interactions between the baseline oxidative state of Hb, possible structural modifications, environmental factors such as the presence of small molecular oxidants, and possibly the presence or absence of specific Hb or heme scavengers such as haptoglobin, hemopexin, or their respective cellular receptors determines the biologic impact of Hb during oxidative-stress conditions (23, 31, 38, 39, 41). It should be kept in mind that different cell types might reflect different responses to Hb or its oxidation products. For example, heme has been identified as a ligand of Toll-like receptor 4 (TLR4) and might thus induce or enhance an inflammatory response in some dedicated cell types (15). Accordingly, other pattern-recognition receptors might display specificity for heme-adducted, oxidized, or cross-linked Hb species. Considering all these factors will help to explain the role of Hb in tissue homeostasis during inflammation, tissue injury, and in hemolytic and vascular diseases.

Acknowledgments

Author Disclosure Statement

References

1. Alayash AI. Oxygen therapeutics: can we tame haemoglobin? *Nat Rev Drug Discov* 3: 152–159, 2004.
2. Alayash AI, Ryan BA, Eich RF, Olson JS, and Cashon RE. Reactions of sperm whale myoglobin with hydrogen peroxide: effects of distal pocket mutations on the formation and stability of the ferryl intermediate. *J Biol Chem* 274: 2029–2037, 1999.

3. Balla J, Jacob HS, Balla G, Nath K, Eaton JW, and Vercellotti GM. Endothelial-cell heme uptake from heme proteins: induction of sensitization and desensitization to oxidant damage. *Proc Natl Acad Sci U S A* 90: 9285–9289, 1993.

4. Boretti FS, Buehler PW, D'Agnillo F, Kluge K, Glaus T, Butt OI, Jia Y, Goede J, Pereira CP, Maggiorini M, Schoedon G, Alayash AI, and Schaer DJ. Sequestration of extracellular hemoglobin within a haptoglobin complex decreases its hypertensive and oxidative effects in dogs and guinea pigs. *J Clin Invest* 119: 2271–2280, 2009.

5. Boykins RA, Buehler PW, Jia Y, Venable R, and Alayash AI. *O*-raffinose crosslinked hemoglobin lacks site-specific chemistry in the central cavity: structural and functional consequences of beta93Cys modification. *Proteins* 59: 840–855, 2005.

6. Boyle JJ, Harrington HA, Piper E, Elderfield K, Stark J, Landis RC, and Haskard DO. Coronary intraplaque hemorrhage evokes a novel atheroprotective macrophage phenotype. *Am J Pathol* 174: 1097–1108, 2009.

7. Buehler PW, Abraham B, Vallelian F, Linnemayr C, Pereira CP, Cipollo JF, Jia Y, Mikolajczyk M, Boretti FS, Schoedon G, Alayash AI, and Schaer DJ. Haptoglobin preserves the CD163 hemoglobin scavenger pathway by shielding hemoglobin from peroxidative modification. *Blood* 113: 2578–2586, 2009.

8. Buehler PW and D'Agnillo F. Toxicological consequences of extracellular hemoglobin: biochemical and physiological perspectives. *Antioxid Redox Signal* 2009.

9. Cashon RE and Alayash AI. Reaction of human hemoglobin HbA0 and two cross-linked derivatives with hydrogen peroxide: differential behavior of the ferryl intermediate. *Arch Biochem Biophys* 316: 461–469, 1995.

10. Cooper CE. Radical producing and consuming reactions of hemoglobin: how can we limit toxicity? *Artif Organs* 33: 110–114, 2009.

11. Cooper CE, Silaghi-Dumitrescu R, Rukengwa M, Alayash AI, and Buehler PW. Peroxidase activity of hemoglobin towards ascorbate and urate: a synergistic protective strategy against toxicity of hemoglobin-based oxygen carriers (HBOCs). *Biochim Biophys Acta* 1784: 1415–1420, 2008.

12. D'Agnillo F and Alayash AI. Redox cycling of diaspirin cross-linked hemoglobin induces G_2/M arrest and apoptosis in cultured endothelial cells. *Blood* 98: 3315–3323, 2001.

13. D'Agnillo F and Alayash AI. A role for the myoglobin redox cycle in the induction of endothelial cell apoptosis. *Free Radic Biol Med* 33: 1153–1164, 2002.

14. Dhanasekaran A, Kotamraju S, Kalivendi SV, Matsunaga T, Shang T, Keszler A, Joseph J, and Kalyanaraman B. Supplementation of endothelial cells with mitochondria-targeted antioxidants inhibit peroxide-induced mitochondrial iron uptake, oxidative damage, and apoptosis. *J Biol Chem* 279: 37575–37587. 2004.

15. Figueiredo RT, Fernandez PL, Mourao-Sa DS, Porto BN, Dutra FF, Alves LS, Oliveira MF, Oliveira PL, Graca-Souza AV, and Bozza MT. Characterization of heme as activator of Toll-like receptor 4. *J Biol Chem* 282: 20221–20229, 2007.

16. Giulivi C and Davies KJ. Hydrogen peroxide-mediated ferrylhemoglobin generation in vitro and in red blood cells. *Methods Enzymol* 231: 490–496, 1994.

17. Graca-Souza AV, Arruda MAB, de Freitas MS, Barja-Fidalgo C, and Oliveira PL. Neutrophil activation by heme: implications for inflammatory processes. *Blood* 99: 4160–4165, 2002.

18. Gramaglia I, Sobolewski P, Meays D, Contreras R, Nolan JP, Frangos JA, Intaglietta M, and van der Heyde HC. Low nitric oxide bioavailability contributes to the genesis of experimental cerebral malaria. *Nat Med* 12: 1417–1422, 2006.

19. Huang L, Wojciechowski G, and Ortiz de Montellano PR. Prosthetic heme modification during halide ion oxidation: demonstration of chloride oxidation by horseradish peroxidase. *J Am Chem Soc* 127: 5345–5353, 2005.

20. Huang L, Wojciechowski G, and Ortiz de Montellano PR. Role of heme-protein covalent bonds in mammalian peroxidases: protection of the heme by a single engineered heme-protein link in horseradish peroxidase. *J Biol Chem* 281: 18983–18938, 2006.

21. Jia Y, Buehler PW, Boykins RA, Venable RM, and Alayash AI. Structural basis of peroxide-mediated changes in human hemoglobin: a novel oxidative pathway. *J Biol Chem* 282: 4894–4907, 2007.

22. Kolodgie FD, Gold HK, Burke AP, Fowler DR, Kruth HS, Weber DK, Farb A, Guerrero LJ, Hayase M, Kutys R, Narula J, Finn AV, and Virmani R. Intraplaque hemorrhage and progression of coronary atheroma. *N Engl J Med* 349: 2316–2325, 2003.

23. Levy A, Asleh R, Blum S, Levy N, Miller-Lotan R, Kalet-Litman S, Anbinder Y, Lache O, Nakhoul F, Asaf R, Farbstein D, Pollak M, Soloveichik Y, Strauss M, Alshiek J, Livshits A, Schwartz A, Awad H, Jad K, and Goldstein H. Haptoglobin: basic and clinical aspects. *Antioxid Redox Signal* 2009.

24. Liu X and Spolarics Z. Methemoglobin is a potent activator of endothelial cells by stimulating IL-6 and IL-8 production and E-selectin membrane expression. *Am J Physiol Cell Physiol* 285: C1036–C1046, 2003.

25. Locher R, Brandes RP, Vetter W, and Barton M. Native LDL induces proliferation of human vascular smooth muscle cells via redox-mediated activation of ERK 1/2 mitogen-activated protein kinases. *Hypertension* 39: 645–650, 2002.

26. Miller YI, Altamentova SM, and Shaklai N. Oxidation of low-density lipoprotein by hemoglobin stems from a heme-initiated globin radical: antioxidant role of haptoglobin. *Biochemistry* 36: 12189–12198, 1997.

27. Miller YI, Smith A, Morgan WT, and Shaklai N. Role of hemopexin in protection of low-density lipoprotein against hemoglobin-induced oxidation. *Biochemistry* 35: 13112–13117, 1996.

28. Nagababu E and Rifkind JM. Formation of fluorescent heme degradation products during the oxidation of hemoglobin by hydrogen peroxide. *Biochem Biophys Res Commun* 247: 592–596, 1998.

29. Nagababu E and Rifkind JM. Heme degradation during autoxidation of oxyhemoglobin. *Biochem Biophys Res Commun* 273: 839–845, 2000.

30. Nagababu E and Rifkind JM. Reaction of hydrogen peroxide with ferrylhemoglobin: superoxide production and heme degradation. *Biochemistry* 39: 12503–12511, 2000.

31. Nielsen MJ, Moller HJ, and Moestrup SK. Hemoglobin and heme scavenger receptors. *Antioxid Redox Signal*. 2009.

32. Reeder BJ, Sharpe MA, Kay AD, Kerr M, Moore K, and Wilson MT. Toxicity of myoglobin and haemoglobin: oxidative stress in patients with rhabdomyolysis and subarachnoid haemorrhage. *Biochem Soc Trans* 30: 745–748, 2002.

33. Reeder BJ, Svistunenko DA, Cooper CE, and Wilson MT. The radical and redox chemistry of myoglobin and hemoglobin:

from in vitro studies to human pathology. *Antioxid Redox Signal* 6: 954–66, 2004.

34. Reiter CD, Wang X, Tanus-Santos JE, Hogg N, Cannon RO 3rd, Schechter AN, and Gladwin MT. Cell-free hemoglobin limits nitric oxide bioavailability in sickle-cell disease. *Nat Med* 8: 1383–1289, 2002.

35. Rother RP, Bell L, Hillmen P, and Gladwin MT. The clinical sequelae of intravascular hemolysis and extracellular plasma hemoglobin: a novel mechanism of human disease. *JAMA* 293: 1653–1662, 2005.

36. Sadrzadeh SM, Graf E, Panter SS, Hallaway PE, and Eaton JW. Hemoglobin: a biologic Fenton reagent. *J Biol Chem* 259: 14354–14356, 1984.

37. Schaer CA, Schoedon G, Imhof A, Kurrer MO, and Schaer DJ. Constitutive endocytosis of CD163 mediates hemoglobin-heme uptake and determines the noninflammatory and protective transcriptional response of macrophages to hemoglobin. *Circ Res* 99: 943–950, 2006.

38. Schaer DJ, Alayash AI, and Buehler PW. Gating the radical hemoglobin to macrophages: the anti-inflammatory role of CD163, a scavenger receptor. *Antioxid Redox Signal* 9: 991–999, 2007.

39. Schaer DJ, Schaer CA, Buehler PW, Boykins RA, Schoedon G, Alayash AI, and Schaffner A. CD163 is the macrophage scavenger receptor for native and chemically modified hemoglobins in the absence of haptoglobin. *Blood* 107: 373–380, 2006.

40. Schaffner A, Rhyn P, Schoedon G, and Schaer DJ. Regulated expression of platelet factor 4 in human monocytes: role of PARs as a quantitatively important monocyte activation pathway. *J Leukoc Biol* 78: 202–209, 2005.

41. Tolosano E, Fagoonee S, Morello N, Vinchi F, and Fiorito V. Heme scavenging and the other facets of hemopexin. *Antioxid Redox Signal* 2009.

42. Vallelian F, Pimenova T, Pereira CP, Abraham B, Mikolajczyk MG, Schoedon G, Zenobi R, Alayash AI, Buehler PW, and Schaer DJ. The reaction of hydrogen peroxide with hemoglobin induces extensive alpha-globin crosslinking and impairs the interaction of hemoglobin with endogenous scavenger pathways. *Free Radic Biol Med* 45: 1150–1158, 2008.

43. Wojciechowski G, Huang L, and Ortiz de Montellano PR. Autocatalytic modification of the prosthetic heme of horseradish but not lactoperoxidase by thiocyanate oxidation products: a role for heme-protein covalent cross-linking. *J Am Chem Soc* 127: 15871–15879, 2005.

Address correspondence to:
Dominik J. Schaer, M.D.
Department of Internal Medicine
University Hospital
CH-8091 Zurich, Switzerland

E-mail: dominik.schaer@usz.ch

This article has been cited by:

1. Olha Yelisyeyeva, Khrystyna Semen, Neven Zarkovic, Danylo Kaminskyy, Olexander Lutsyk, Volodymyr Rybalchenko. 2012. Activation of aerobic metabolism by Amaranth oil improves heart rate variability both in athletes and patients with type 2 diabetes mellitus. *Archives Of Physiology And Biochemistry* 1-11. [CrossRef]

2. Alessandro Pessione, Cristina Lamberti, Luca Cocolin, Simona Campolongo, Alexander Grunau, Sonia Giubergia, Leo Eberl, Kathrin Riedel, Enrica Pessione. 2012. Different protein expression profiles in cheese and clinical isolates of Enterococcus faecalis revealed by proteomic analysis. *PROTEOMICS* **12**:3, 431-447. [CrossRef]

3. Jay F. Storz, Roy E. Weber, Angela Fago. 2012. Oxygenation properties and oxidation rates of mouse hemoglobins that differ in reactive cysteine content. *Comparative Biochemistry and Physiology Part A: Molecular & Integrative Physiology* **161**:2, 265-270. [CrossRef]

4. Sofia Morais, Tomé Silva, Odete Cordeiro, Pedro Rodrigues, Derrick R Guy, James E Bron, John B Taggart, J Gordon Bell, Douglas R Tocher. 2012. Effects of genotype and dietary fish oil replacement with vegetable oil on the intestinal transcriptome and proteome of Atlantic salmon (Salmo salar). *BMC Genomics* **13**:1, 448. [CrossRef]

5. S. N. Balaji, Vishal Trivedi. 2011. Extracellular Methemoglobin Mediated Early ROS Spike Triggers Osmotic Fragility and RBC Destruction: An Insight into the Enhanced Hemolysis During Malaria. *Indian Journal of Clinical Biochemistry* . [CrossRef]

6. Bindu Abraham, Wayne Hicks, Yiping Jia, Jin Hyen Baek, Jeffery L. Miller, Abdu I. Alayash. 2011. Isolated Hb Providence #82Asn and #82Asp Fractions Are More Stable than Native HbA 0 under Oxidative Stress Conditions. *Biochemistry* 111021094205009. [CrossRef]

7. Wei Zhang, Kunping Yan, Penggao Dai, Jingjing Tian, Hongli Zhu, Chao Chen. 2011. A Novel Hemoglobin-Based Oxygen Carrier, Polymerized Porcine Hemoglobin, Inhibits H2O2-Induced Cytotoxicity of Endothelial Cells. *Artificial Organs* no-no. [CrossRef]

8. Paul W. Buehler, Felice D'AgnilloAnimal Models and Oxidative Biomarkers to Evaluate Preclinical Safety of Extracellular Hemoglobins 391-411. [CrossRef]

9. C.E. Angulo-Valadez, M.C. Reyes-Becerril, G.M.J. Romero, R. Cepeda-Palacios, D.R. López-Aguilar, T. Zenteno, F. Ascencio. 2011. Antioxidant enzymes in erythrocytes from goats seropositive to the sheep nose bot fly (Oestrus ovis L., Diptera: Oestridae) infection. *Veterinary Parasitology* . [CrossRef]

10. Harriet Mörtstedt, Marina C. Jeppsson, Giovanni Ferrari, Bo A.G. Jönsson, Monica H. Kåredal, Christian H. Lindh. 2011. Strategy for identification and detection of multiple oxidative modifications within proteins applied on persulfate-oxidized hemoglobin and human serum albumin. *Rapid Communications in Mass Spectrometry* **25**:2, 327-340. [CrossRef]

11. Weiguang Li, Yonghong Wu, Changhong Ren, Yiming Lu, Yan Gao, Xiaofei Zheng, Chenggang Zhang. 2011. The activity of recombinant human neuroglobin as an antioxidant and free radical scavenger. *Proteins: Structure, Function, and Bioinformatics* **79**:1, 115-125. [CrossRef]

12. Sonja Reiland, Jonas Grossmann, Katja Baerenfaller, Peter Gehrig, Adriano Nunes-Nesi, Alisdair R. Fernie, Wilhelm Gruissem, Sacha Baginsky. 2011. Integrated proteome and metabolite analysis of the de-etiolation process in plastids from rice (Oryza sativa L.). *PROTEOMICS* n/a-n/a. [CrossRef]

13. Brandon J. Reeder . 2010. The Redox Activity of Hemoglobins: From Physiologic Functions to Pathologic Mechanisms. *Antioxidants & Redox Signaling* **13**:7, 1087-1123. [Abstract] [Full Text HTML] [Full Text PDF] [Full Text PDF with Links]